Noname manuscript No.
(will be inserted by the editor)

Squdel function: square wave approximation without ringing

M. Fernández Guasti

the date of receipt and acceptance should be inserted later

Abstract A function that is well suited to describe a square wave as well as a sequence of delta functions is presented. The squdel function has a closed rational form instead of a series approximation. Bandwidth limitations are readily incorporated in this function without producing undesirable ringing artifacts. The squdel function is infinitely differentiable and analytic for a squareness parameter as close as required to the square function provided that the limit is not taken. Even its Fourier series decomposition does not exhibit overshooting when truncated. Two dimensional soft pixel structures are shown to be economically modeled with this function.

Keywords Wave synthesis · Square wave · Dirac comb · Limited bandwidth · Ringing · Pixel shape

1 Introduction

The square function is usually defined in terms of discontinuous functions such as the sign or Heaviside functions. Representations in terms of differentiable/holomorphic functions are usually expressed in terms of real/complex Fourier series. A finite number of terms in the infinite series account for experimental realizations with limited bandwidth of real life devices. These series exhibit the Gibbs phenomenon that involves a signal overshoot at a jump discontinuity [13]. This undesirable phenomenon gives rise to ringing artifacts in signal processing that show up, for example, as ghosts near sharp edges in digital image processing [10]. Coherent imaging also exhibits ringing due to diffraction of sharp edges [11]. Theoretically, the Gibbs phenomenon

e-mail: mfg@xanum.uam.mx, url: https://luz.izt.uam.mx

Lab. de Óptica Cuántica, Depto. de Física,
Universidad A. Metropolitana - Iztapalapa,
09340 México D.F., Ap. postal. 55-534, MEXICO

is reduced by using a modified Fourier series summation [15]. In experimental devices, ringing is minimized with appropriate filtering in electronic circuits [1] and apodization in optical systems [2].

Closed-form approximations to the square wave can be generated by the odd nth real root of the sine/cosine functions, i.e. $\sin^{\frac{1}{n}}(\omega t)$ [3]. These functions produce a sharp transition between the two levels of the square function but fail to produce a flat region unless very high order odd roots (say above the 51^{st} root) are used. However, the rise and fall times are then also greatly increased. Another alternative is to synthesize each step with an exponential function with real argument [6] or a hyperbolic tangent function [8]. This approach embraces various possibilities because it permits the control of the duty cycle as well as different rise/fall times. Although quite adequate for a step or a few pulses, this scheme is less well suited for modeling an extended or infinite wave train.

The trigonometric identity

$$\cos\left[\arctan\left(\frac{B}{A}\tan\phi\right)\right] = \frac{A\cos\phi}{\sqrt{A^2\cos^2\phi + B^2\sin^2\phi}},$$

has been invoked to describe a classical indeterminacy of the amplitude and phase functions in a one dimensional oscillating system with possibly time dependent parameters [5]. This study gave rise to the definition of the squdel function presented here in section 2. A square function, a comb and a sampling function can be described with this function. A continuous transformation between these limit cases is achieved via a single real parameter in the squdel function. This function has a threefold advantage as an approximation to a square wave: i) It has a closed rational form. ii) It does not exhibit the typical overshoot of truncated Fourier series. iii) The finite slope due to bandwidth limitations is modeled by the function without producing unwanted ringing effects. These properties are described in section 3. The Fourier series expansion of the squdel function is tackled in section 4. Several interesting inequalities are conjectured in this section. Conclusions and some applications are sketched in the last section.

2 Squdel function

The *squdel sine* function is a real function of real variable $\mathrm{sqd}_s : \mathbb{R} \to \mathbb{R}$, defined by

$$\mathrm{sqd}_s(t) := \frac{\sin(\omega t)}{\sqrt{\sin^2(\omega t) + \kappa^2\cos^2(\omega t)}}. \tag{1}$$

where the positive sign of the square root is enforced and $\omega, \kappa \in \mathbb{R}$. In terms of the double angle in the denominator,

$$\mathrm{sqd}_s(t,\omega,\kappa) = \frac{\sin(\omega t)}{\sqrt{\left(\frac{1+\kappa^2}{2}\right) - \left(\frac{1-\kappa^2}{2}\right)\cos(2\omega t)}}. \tag{2}$$

Similarly, the *squdel cosine* function is defined as

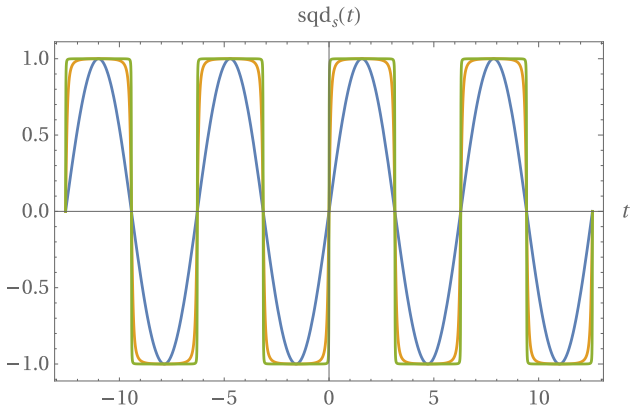

Fig. 1 Squdel sine function given by Eq. (1) for $\omega = 1$ with $\kappa = 1$ (sine function), $\kappa = .1$ (intermediate blunt corners), $\kappa = .01$ (sharper corners).

$$\mathrm{sqd}_c\left(t,\omega,\kappa\right) := \frac{\cos\left(\omega t\right)}{\sqrt{\kappa^2\sin^2\left(\omega t\right)+\cos^2\left(\omega t\right)}}. \tag{3}$$

In terms of the double angle, this function exhibits a sign change within the root with respect to the squdel sine function,

$$\mathrm{sqd}_c\left(t,\omega,\kappa\right) = \frac{\cos\left(\omega t\right)}{\sqrt{\left(\frac{1+\kappa^2}{2}\right)+\left(\frac{1-\kappa^2}{2}\right)\cos\left(2\omega t\right)}}.$$

The squdel sine function has odd parity whereas the squdel cosine function has even parity. The subscript is dropped for economy, if the context does not give rise to confusion.

For $\kappa = 1$, the squdel sine function is simply the sinusoidal function $\sin\left(\omega t\right)$. In the $\kappa \to 0$ limit,

$$\lim_{\kappa\to 0}\frac{\sin\phi}{\sqrt{\sin^2\left(\omega t\right)+\kappa^2\cos^2\left(\omega t\right)}} = \begin{cases} \frac{\sin\phi}{\sqrt{\sin^2\phi}} = 1 & \text{for } 0 \le \phi \le \pi, \bmod 2\pi \\ \frac{\sin\phi}{\sqrt{\sin^2\phi}} = -1 & \text{for } \pi \le \phi \le 2\pi, \bmod 2\pi \end{cases},$$

a square function is thus obtained. In the intermediate cases $0 < \kappa < 1$, the squdel sine function resembles a square function but the transition takes place in a finite time and the function has blunt corners as shown in figure 1. Therefore, a square function can be approximated by a squdel function without having to restore to a series approximation. No truncation is required since the squdel function has a closed-form expression. All that is necessary is to set the parameter κ at the appropriate value according to the desired degree of approximation. A remarkable feature is that regardless of the value of κ, there are no oscillations near the edges, not even small ones as we shall prove in the next section.

For $\kappa > 1$, the squdel function exhibits periodic peaks that become narrower as the value of κ is increased. The square of the squdel function is similar to a comb structure with finite width peaks as shown in figure 2. The $\kappa \to \infty$ limit produces a

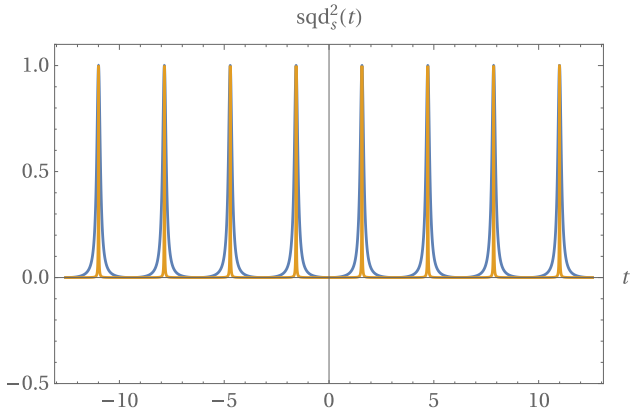

Fig. 2 Squdel sine function squared for $\omega = 1, \kappa = 10$ (broader peaks) and $\kappa = 100$ (narrower peaks).

comb with maxima equal to one. If the square of the squdel function is multiplied by κ times the normalization factor $\frac{\omega}{\pi}$, the area under the curve is 1 in the limit of large κ. The $\lim_{\kappa\to\infty}\left(\frac{\kappa\omega}{\pi}\,\mathrm{sqd}_s^2\right)$ reproduces a sampling function, also referred to as Dirac comb or Shah function. The same is true for the squdel cosine function but shifted by $\frac{\pi}{2}$ with respect to the sqd_s function.

3 Differentiability and finite bandwidth

The first derivative of the squdel sine function is

$$\frac{d}{dt}\mathrm{sqd}_s\,(t) = \frac{\kappa^2\omega\cos(\omega t)}{\left(\left(\frac{1+\kappa^2}{2}\right) - \left(\frac{1-\kappa^2}{2}\right)\cos\left(2\omega t\right)\right)^{3/2}}. \tag{4}$$

Whereas its second derivative is

$$\frac{d^2}{dt^2}\mathrm{sqd}_s\,(t) = -\frac{\kappa^2\omega^2\sin(\omega t)\left(\left(2-\kappa^2\right) + \left(1-\kappa^2\right)\cos(2\omega t)\right)}{\left(\left(\frac{1+\kappa^2}{2}\right) - \left(\frac{1-\kappa^2}{2}\right)\cos\left(2\omega t\right)\right)^{5/2}}. \tag{5}$$

The nth derivative involves a denominator of the form

$$\left(\left(\frac{1+\kappa^2}{2}\right) - \left(\frac{1-\kappa^2}{2}\right)\cos\left(2\omega t\right)\right)^{(2n+1)/2}.$$

The minimum value for this expression is 1 for $\kappa^2 \geq 1$ and κ^2 for $\kappa^2 \leq 1$. The denominator is thus never zero provided that $\kappa \neq 0$. The sqd_s function is therefore infinitely differentiable provided that $\kappa \neq 0$. The Taylor series

$$\sum_{n=0}^{\infty} \frac{\mathrm{sqd}_s^{(n)}(t_0)}{n!}\,(t-t_0)^n$$

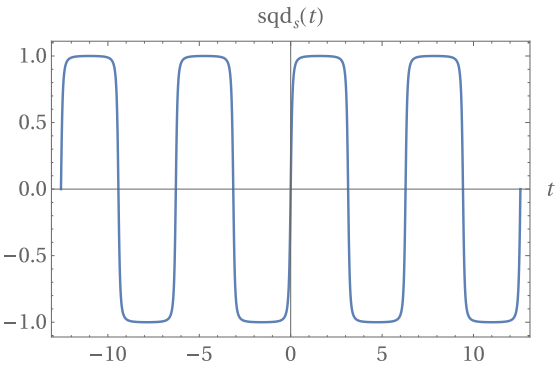

Fig. 3 Squdel sine function with $\kappa = .1$ The cutoff frequency is $\omega_c = 10\,\omega$.

converges to the function at every point so that the function is analytic in the real line provided that $\kappa \neq 0$.

From (5), the maximum slope of the sqd_s function is obtained at the inflexion point $t = 0$, mod π. The maximum (minimum) slope, obtained from the first order derivative is then

$$\frac{d}{dt}\mathrm{sqd}_s\left(t,\omega,\kappa\right)\Big|_{t=0} = -\frac{d}{dt}\mathrm{sqd}_s\left(t,\omega,\kappa\right)\Big|_{t=\pi} = \frac{\omega}{\kappa}.$$

If ω_c is the cutoff frequency of the system, the maximum slope of a sinusoidal signal with ω_c frequency is

$$\frac{d}{dt}\sin\left(\omega_c t\right)\Big|_{t=0} = \omega_c \cos\left(\omega_c t\right)|_{t=0} = \omega_c.$$

Equating the slopes of these two expressions,

$$\kappa = \frac{\omega}{\omega_c}.$$

This result provides a simple and efficient way to evaluate an analytical approximation for a square wave. Given a square wave with frequency ω and a system with ω_c cutoff frequency, the square wave propagating within the system is given by

$$\mathrm{sqd}_s\left(t,\omega,\frac{\omega}{\omega_c}\right) = \frac{\sin\left(\omega t\right)}{\sqrt{\sin^2\left(\omega t\right) + \frac{\omega^2}{\omega_c^2}\cos^2\left(\omega t\right)}}. \tag{6}$$

This squdel function exhibits the maximum slope at the transition between the two states that propagate without significant attenuation through the system. A squdel wave with angular frequency ω propagating in a system with ten times higher cutoff frequency $\omega_c = 10\,\omega$ ($\kappa = 0.1$), is depicted in figure 3. Equating the first derivative to zero, maxima and minima are obtained for $\omega t = \frac{\pi}{2}$ mod π, regardless of the value of κ. There is only one maximum in the $(0, \pi)$ interval at $\frac{\pi}{2}$, thus, the squdel function does not exhibit ringing. It is therefore possible to account for a finite bandwidth signal without any ringing. To further elucidate this point, a close up of the squdel function for different values of κ is shown in figure 4. The plot of one corner of

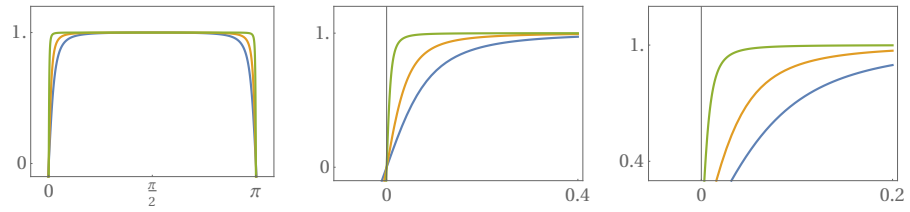

Fig. 4 Detail of squdel sine function with $\kappa = .1, .05, .01$. Frames with increasing detail from left to right reveal no ringing even at very large magnification.

the function is shown with increasing level of detail. The function does not exhibit any ringing regardless of the value of the parameter κ, consistent with the results obtained from the function derivatives. Even at the largest magnification, the plot shows a smooth curve without any local maxima.

4 Fourier series

The Fourier series expansion of the squdel sine function is

$$\begin{aligned}\mathrm{sqd}_s\,(t) = {} & 2\kappa\frac{{}_2F_1(-\tfrac{1}{2},\tfrac{1}{2};1;x) - {}_2F_1(\tfrac{1}{2},\tfrac{1}{2};1;x)}{(1-\kappa^2)}\sin(t) \\ & + 2\kappa\frac{\left(7\kappa^2+1\right){}_2F_1(-\tfrac{1}{2},\tfrac{1}{2};1;x) - \left(3\kappa^2+5\right){}_2F_1(\tfrac{1}{2},\tfrac{1}{2};1;x)}{3\,(1-\kappa^2)^2}\sin(3t) \\ & + 2\kappa\frac{\left(43\kappa^4+82\kappa^2+3\right){}_2F_1(-\tfrac{1}{2},\tfrac{1}{2};1;x) - \left(15\kappa^4+74\kappa^2+39\right){}_2F_1(\tfrac{1}{2},\tfrac{1}{2};1;x)}{15\,(1-\kappa^2)^3}\sin(5t) \\ & + \mathcal{O}^+\left(\sin(7t)\right)\end{aligned}$$

where ${}_2F_1$ is the hypergeometric function and $x = 1 - \frac{1}{\kappa^2}$. Many common functions can be expressed in terms of the hypergeometric function depending on the values of its argument. Some examples are the logarithm, inverse trigonometric functions, Legendre and other polynomials or the elliptic integral functions. For $1 < \kappa < \infty$, where the squdel function resembles a comb like structure, the argument $0 < x < 1$ is positive. The hypergeometric function ${}_2F_1(\pm\frac{1}{2},\frac{1}{2};1;x)$ is then equal to $K\left(\sqrt{x}\right)$ (positive sign) or $E\left(\sqrt{x}\right)$ (negative sign), the complete elliptic integrals of the first and second kinds. The first few components of the Fourier decomposition are shown in figure (5). Notice that for $\kappa \neq 0$, the amplitude of higher order components always decreases, thus the Gibbs phenomenon is not present.

The limit when $\kappa \to 0$ has to be evaluated with care since the limit of the hypergeometric function ${}_2F_1(-\frac{1}{2},\frac{1}{2};1;x)$ when $x \to -\infty$ is ∞. However, the limit of the product of κ times ${}_2F_1(-\frac{1}{2},\frac{1}{2};1;1-\frac{1}{\kappa^2})$ when $\kappa \to 0$ is $\frac{2}{\pi}$. The first terms in this limit are

$$\lim_{\kappa\to 0}\mathrm{sqd}_s\,(t) = \frac{4}{\pi}\sin(t) + \frac{4}{3\pi}\sin(3t) + \frac{4}{5\pi}\sin(5t) + \ldots,$$

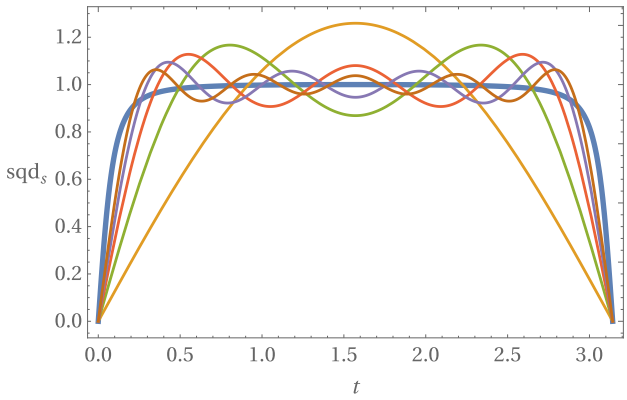

Fig. 5 Squdel sine function with $\kappa = .1$ in the $(0, \pi)$ interval. Decreasing peak amplitudes at the side extremes of the Fourier components at $\omega, 3\omega, 5\omega, 7\omega$ and 9ω evince that the Gibbs phenomenon is not present.

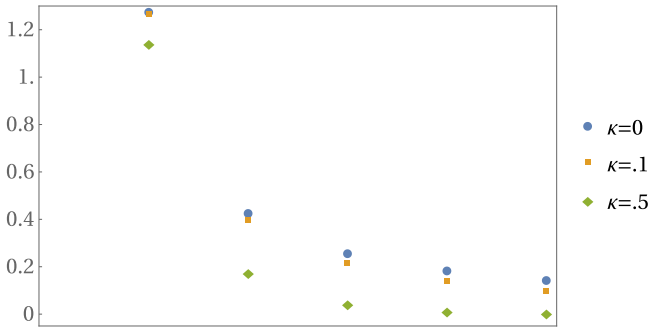

Fig. 6 Squdel Fourier coefficients at $\omega, 3\omega, 5\omega, 7\omega$ and 9ω arguments of the sine function for different values of κ.

thus reproducing the Fourier series of the square function. We conjecture that the Fourier coefficients of the squdel expansion with $0 < \kappa < 1$ are always smaller than the Fourier coefficients of the square function. For example, for the leading term

$$2\kappa \frac{{}_2F_1(-\frac{1}{2}, \frac{1}{2}; 1; x) - {}_2F_1(\frac{1}{2}, \frac{1}{2}; 1; x)}{(1-\kappa^2)} < \frac{4}{\pi},$$

whereas for the second term

$$2\kappa \frac{\left(7\kappa^2+1\right) {}_2F_1(-\frac{1}{2}, \frac{1}{2}; 1; x) - \left(3\kappa^2+5\right) {}_2F_1(\frac{1}{2}, \frac{1}{2}; 1; x)}{3\left(1-\kappa^2\right)^2} < \frac{4}{3\pi},$$

and so on. This behaviour is shown in figure 6 for the first few terms. From the figure, it can be seen that the coefficients' magnitude decrease is more pronounced as κ becomes larger. I.e. inequalities of the type $2\kappa_b \frac{{}_2F_1(-\frac{1}{2}, \frac{1}{2}; 1; x_b) - {}_2F_1(\frac{1}{2}, \frac{1}{2}; 1; x_b)}{\left(1-\kappa_b^2\right)} < 2\kappa_a \frac{{}_2F_1(-\frac{1}{2}, \frac{1}{2}; 1; x_a) - {}_2F_1(\frac{1}{2}, \frac{1}{2}; 1; x_a)}{(1-\kappa_a^2)}$ for $\kappa_b > \kappa_a$ should be fulfilled by all terms.

The Fourier coefficients of the squdel functions may be considered as an alternative to square wave Fourier coefficients weighed with the sinc functions introduced by

the σ Lanczos kernel factors [12]. However, it should be noted that while the sigma factors reduce the ringing artifacts, the squdel Fourier series coefficients completely extinguish the Gibbs phenomenon. Nonetheless, it should be stressed that a series expansion of the squdel function is unnecessary. An asset of this function is that it can account for a finite bandwidth via the parameter κ while retaining its closed-form.

5 Concluding remarks

The squdel sine and cosine functions have been defined and their fundamental properties described. The squdel tangent and other trigonometric squdel functions can be readily obtained from the functions presented here. These C^∞ real functions are analytic and prove adequate to describe the square wave and comb functions as well as their propagation in limited bandwidth systems. In this latter case, a closed-form is retained. Therefore, there is no need to consider the truncated Fourier series of the function even if the system has a cutoff frequency. An important asset is that neither the closed-form of the function nor its truncated Fourier series exhibit the overshooting Gibbs phenomenon.

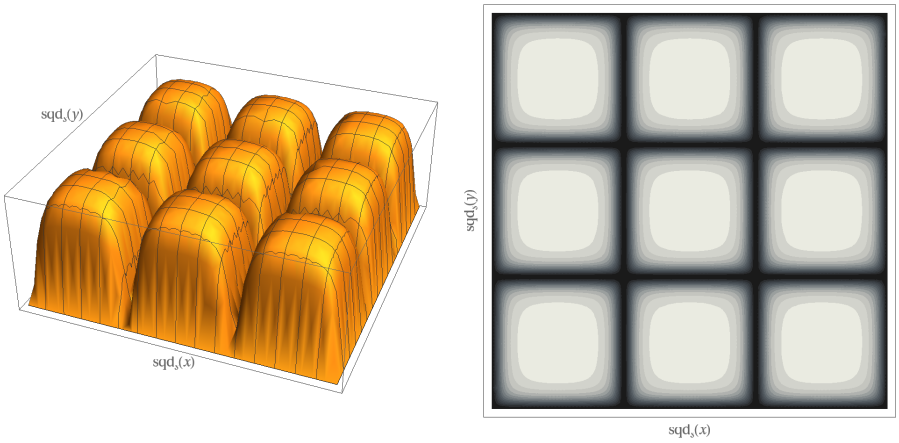

Fig. 7 Pixel simulation with a squdel soft profile emission (or transmission) intensity. Left: 3D plot where the vertical axis represents intensity; Right: corresponding contour plot.

Digital screen reticules are usually described by square or rectangular figures. However, diffraction patterns from such structures in real life devices [9] reveal that the square corners are usually slightly blunt [7]. The actual shape is more closely described by a squircle hard aperture [4]. A two dimensional squdel function can be used to model a similar shape to the squircle but with a more realistic soft aperture as shown in figure 7. The $\mathrm{sqd}_s\left(x, \omega_x, \kappa_x\right) \mathrm{sqd}_s\left(y, \omega_y, \kappa_y\right)$ function describes a two dimensional rectangular pixel array with $\frac{2\pi}{\omega_x}, \frac{2\pi}{\omega_y}$ periodicities. The κ_x, κ_y parameters sharpen or blur the pixel's contours.

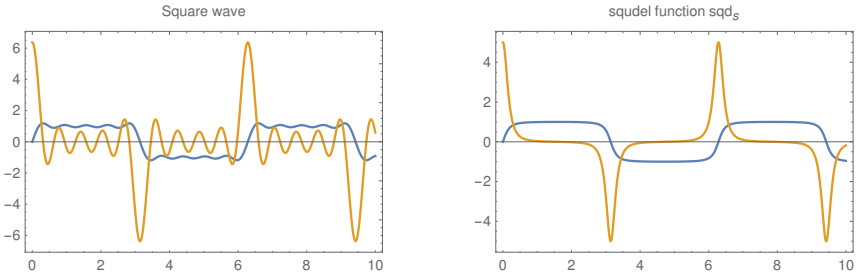

Fig. 8 Differentiation signal processor. Bandwidth limited input function (blue) and derivative function (orange). Square wave truncated series on the left; Squdel function with $\kappa = 0.1$ on the right. The squdel derivative signal is noise free.

In order to show the advantage of the squdel function against the square wave for signal processing system analysis, consider a differentiator circuit with 10 times larger bandwidth than the signal frequency. Allow for a square wave input that due to a brick-wall cutoff frequency is usually represented in Fourier series truncated after the 5th term at frequency 9ω. The ringing of the truncated series produces considerable noise in the derivative signal as shown in figure 8. In contrast, let the bandwidth limited square wave be represented by a squdel function (6) with $\kappa = \frac{\omega}{\omega_c} = \frac{1}{10} = 0.1$. The derivative of this function (4), exhibits the peaks due to the squdel square wave transition, but has no noise since there is no ringing in the bandwidth limited squdel function. The crucial difference between the two procedures being that the squdel function can be bandwidth limited without having to restore to a truncated series approach.

The complex shearlet transform (CST) involves a Fourier transform where the window function is a weighing factor which does not exhibit the Gibbs effect [14]. It will be interesting to explore the possibility of integrating the present formalism into these recent digital processing algorithms.

References

1. Allen, R., Mills, D.: Signal Analysis: Time, Frequency, Scale, and Structure. Wiley (2004).
2. Bass, M., et al. (eds.): Handbook of Optics, vol. 2, 2nd edn. McGraw-Hill Publishing (1995)
3. Diamant, R., Fernández-Guasti, M.: Novel method to compute high reflectivity of multilayered mirrors with rugate features. OSA (2013).
4. Fernández-Guasti, M.: Analytic geometry of some rectilinear figures. Int. Jour. of Math. Ed. in Sci. & Tech. **23**(6), 895–901 (1992).
5. Fernández-Guasti, M.: Indeterminacy of amplitude and phase variables in classical dynamical systems: the harmonic oscillator. Europhysics Letters **74**(6), 1013–1019 (2006).
6. Fernández-Guasti, M., Chim, A.T.: Charge motion under ultrafast harmonic wave switching. In: M. Martinez-Mares, J.A. Moreno-Razo (eds.) Symposium on Condensed Matter Physics, *IV Mexican Meeting on Experimental and Theoretical Physics*, vol. 1319, p. 57–69. AIP conference proceedings (2010).
7. Fernández-Guasti, M., Cobarrubias, A.M., Carrillo, F.R., Cornejo-Rodríguez, A.: LCD pixel shape and far field diffraction patterns. Optik **116**, 265–269 (2005).
8. Fernández-Guasti, M., Gil-Villegas, A., Diamant, R.: Ermakov equation arising from electromagnetic fields propagating in 1D. Revista Mexicana de Física **46**, 530–535 (2000).

9. Fernández-Guasti, M., Heredia, M.D.L.C.: Diffraction pattern of a circle/square aperture. Journal of Modern Optics **40**(6), 1073–1080 (1993).
10. Glassner, A.: Principles of digital image synthesis: Vol. 1. Kaufmann (1995).
11. Goodman, J.W.: Introduction to Fourier Optics, 3rd edition edn. Roberts and Company (2005)
12. Hamming, R.W.: Numerical Methods for Scientists and Engineers, 2nd edn. Dover (1986)
13. Hewitt E., Hewitt R. E.: The Gibbs-Wilbraham phenomenon: An episode in fourier analysis. Archive for History of Exact Sciences **21**(2), 129–160 (1979).
14. Liu, S., Shi, M., Zhu, Z., Zhao, J.: Image fusion based on complex-shearlet domain with guided filtering. Multidimensional Systems and Signal Processing **28**(1), 207–224 (2017).
15. Wu, Q., Merchant, F., Castleman, K.: Microscope Image Processing. Elsevier Science (2010).